2-28-2019

Ultrasound-triggered antibiotic release from PEEK clips to prevent spinal fusion infection: Initial evaluations.

Lauren J. Delaney
Thomas Jefferson University, lauren.delaney@jefferson.edu

Daniel MacDonald
Drexel University

Jay Leung
Drexel University

Keith Fitzgerald
Thomas Jefferson University, keith.fitzgerald@jefferson.edu

Alex M. Sevit
Drexel University

See next page for additional authors

Authors
Lauren J. Delaney, Daniel MacDonald, Jay Leung, Keith Fitzgerald, Alex M. Sevit, John R. Eisenbrey, Neil Patel, Flemming Forsberg, Christopher K. Kepler, Taolin Fang, Steven M. Kurtz, and Noreen J. Hickok

Acta Biomaterialia xxx (xxxx) xxx

Contents lists available at ScienceDirect

Acta Biomaterialia

journal homepage: www.elsevier.com/locate/actabiomat

Ultrasound-triggered antibiotic release from PEEK clips to prevent spinal fusion infection: Initial evaluations ☆

Lauren J. Delaney [a], Daniel MacDonald [b], Jay Leung [b], Keith Fitzgerald [c], Alex M. Sevit [b], John R. Eisenbrey [a], Neil Patel [c], Flemming Forsberg [a], Christopher K. Kepler [c,d], Taolin Fang [c,d], Steven M. Kurtz [b,e], Noreen J. Hickok [c,*]

[a] Department of Radiology, Thomas Jefferson University, 132 S. 10th Street, Philadelphia, PA 19107, USA
[b] School of Biomedical Engineering, Science and Health Systems, Drexel University, 3141 Chestnut Street, Philadelphia, PA 19104, USA
[c] Department of Orthopaedic Surgery, Thomas Jefferson University, 1015 Walnut Street, Philadelphia, PA 19107, USA
[d] The Rothman Institute, Thomas Jefferson University, 925 Chestnut Street, Philadelphia, PA 19107, USA
[e] Exponent, Inc., 3440 Market Street Suite 600, Philadelphia, PA 19104, USA

ARTICLE INFO

Article history:
Received 25 September 2018
Received in revised form 21 February 2019
Accepted 26 February 2019
Available online xxxx

Keywords:
Vancomycin
Polyether ether ketone PEEK
Ultrasound
Staphylococcus aureus
Spine

ABSTRACT

Despite aggressive peri-operative antibiotic treatments, up to 10% of patients undergoing instrumented spinal surgery develop an infection. Like most implant-associated infections, spinal infections persist through colonization and biofilm formation on spinal instrumentation, which can include metal screws and rods for fixation and an intervertebral cage commonly comprised of polyether ether ketone (PEEK). We have designed a PEEK antibiotic reservoir that would clip to the metal fixation rod and that would achieve slow antibiotic release over several days, followed by a bolus release of antibiotics triggered by ultrasound (US) rupture of a reservoir membrane. We have found using human physiological fluid (synovial fluid), that higher levels (100–500 μg) of vancomycin are required to achieve a marked reduction in adherent bacteria vs. that seen in the common bacterial medium, trypticase soy broth. To achieve these levels of release, we applied a polylactic acid coating to a porous PEEK puck, which exhibited both slow and US-triggered release. This design was further refined to a one-hole or two-hole cylindrical PEEK reservoir that can clip onto a spinal rod for clinical use. Short-term release of high levels of antibiotic (340 ± 168 μg), followed by US-triggered release was measured (7420 ± 2992 μg at 48 h). These levels are sufficient to prevent adhesion of *Staphylococcus aureus* to implant materials. This study demonstrates the feasibility of an US-mediated antibiotic delivery device, which could be a potent weapon against spinal surgical site infection.

Statement of Significance

Spinal surgical sites are prone to bacterial colonization, due to presence of instrumentation, long surgical times, and the surgical creation of a dead space (≥5 cm^3) that is filled with wound exudate. Accordingly, it is critical that new approaches are developed to prevent bacterial colonization of spinal implants, especially as neither bulk release systems nor controlled release systems are available for the spine. This new device uses non-invasive ultrasound (US) to trigger bulk release of supra-therapeutic doses of antibiotics from materials commonly used in existing surgical implants. Thus, our new delivery system satisfies this critical need to eradicate surviving bacteria, prevent resistance, and markedly lower spinal infection rates.

1. Introduction

Placement of implants, instrumentation, and/or bone supplementation are critical to orthopaedics with implant-associated infection an infrequent, but devastating complication. The incidence of post-surgical infections depends on the site, and ranges from <1 to 2% for joint replacements [1] and up to 10% for spinal

☆ Part of the Drug Delivery for Musculoskeletal Applications Special Issue, edited by Robert S. Hastings and Professor Johnna S. Temenoff.

* Corresponding author at: Department of Orthopaedic Surgery, Sidney Kimmel Medical College, Thomas Jefferson University, 1015 Walnut St., Ste. 501, Philadelphia, PA 19107, United States.
E-mail address: Noreen.Hickok@jefferson.edu (N.J. Hickok).

https://doi.org/10.1016/j.actbio.2019.02.041
1742-7061/

surgeries [2]. Unfortunately, infection rates also depend on the health of the patient and are expected to increase among the aging, diabetic, obese, and those with metabolic syndrome and other diseases/treatments that affect immune status [3].

Instrument-associated infections which exhibit attenuated immune surveillance arise from bacterial biofilms. These biofilms exhibit reduced responses to antibiotics due to bacterial sequestration, changes in gene expression, and ultimately biofilm formation [4]. Thus, we and others have sought to eradicate bacteria early to prevent biofilm formation and the subsequent seeding of new infections. Current antibacterial systems encompass release of silver nanoparticles [5,6], bioactive antibacterial surfaces including those with long-term, permanent antimicrobial activity [7–9], and controlled antibiotic release systems [10–12]. In the spine, prophylaxis is achieved by inclusion of 1–2 g of vancomycin (VAN) powder during closure [13] to sterilize the site post-surgically. The outcome of this procedure is mixed since VAN reduces the number of infections associated with Gram-positive bacteria (such as the *Staphylococci*), but the number of infections attributed to Gram-negative bacteria may increase [14].

Like other implant-associated infections [15], it is likely that spinal instrumentation (e.g., metal screws, rods, and cages, usually made of porous metal or of polyether ether ketone(PEEK) [16])-associated infections persist through bacterial colonization and biofilm formation. Interestingly, unlike the joint, spinal infections are more often successfully treated by aggressive antibiotic treatments [17]. However, failure to effectively treat an infection can be life threatening, as spinal instrumentation may be required for spinal stability precluding removal.

In the spine, the metal instrumentation exists at the interface of muscle and bone, and at least initially is bathed in post-operative wound fluid. This wound fluid may influence bacterial properties as we and others have shown that methicillin-sensitive *Staphylococcus aureus* (MSSA), methicillin-resistant *Staphylococcus aureus* (MRSA), and *Staphylococcus epidermidis* form >100 μm proteinaceous aggregates and biofilms in blood and synovial fluid (SynF) [18–20]. Aggregation appears to be dependent on the presence of extracellular matrix proteins, including fibrin [19]. Interestingly, fibrous aggregates in blood, as well as surface-bound biofilms, can be permeabilized through application of ultrasound (US), enhancing drug access and efficacy [21–23]. Specifically, US enhances tissue penetration and this penetration can be further enhanced by mechanical disruption of drug-containing nano- and micro-particles, and micelles [24–27]. US-triggered cavitation and rupture of these microbubbles and micelles is well-characterized [28–35], with recent applications for targeted drug delivery [36–39]. These drug-containing bubbles include thin-shelled polymer [40] and polylactic acid (PLA) [41,42] microbubbles, which are tunable for response to focused US in a drug delivery setting and we will use this property in our design.

Thus, we hypothesized that application of US would mechanically rupture a PLA membrane coating a clip with a reservoir. We then suggested that this insonation would cause streaming of drugs out of the reservoir, to result in a non-invasive release of supratherapeutic levels of VAN (Fig. 1). We chose to characterize VAN in this setting as it is already used prophylactically in spinal surgery [13,14,43]. To evaluate these hypotheses, we followed an iterative design process in order to arrive at a clinically-relevant prototype device. We first determined the free VAN concentration that would be required to maintain sterility of the PEEK device in the face of an MSSA challenge as a function of ideal media or physiological fluid. We next examined if milligram amounts of VAN could be sealed into and released from a model porous PEEK puck (First Generation). It was important in this early stage to determine the overall feasibility of the US-triggered release response from a PEEK device. We then built upon our findings with these first generation devices to design more clinically-relevant bulk antibiotic reservoirs in C-shaped clips (Second Generation), and evaluated release characteristics from these refined devices both *in vitro* and in an *ex vivo* animal model.

2. Materials and methods

2.1. Fabrication Conditions

PEEK discs were additively manufactured using a PEEKMed filament (Apium Additive Technologies, Karlsruhe, Germany) using an Indmatec HPP 155/Gen 2 3D printer (Apium Additive Technologies). The discs were printed with a 0.4 mm nozzle at a speed of 1500 mm/min and a layer thickness of 0.1 mm. The filament extruder temperature was 405 °C and print bed temperature 100 °C. The printing process of the disc produced two different surface finishes of the disc faces: one smooth (the face in contact with the glass print bed) and one with a rougher surface finish. For the strain growth and biofilm formation experiments, we used the smooth face of the discs. Tissue culture polystyrene (PS, Corning Costar, Fisher Scientific, Hampton, NH) was used as a control. All surfaces were sterilized by incubation in 70% ethanol in water and 15 min exposure to UV light.

2.2. Strain growth and biofilm formation

Two strains of methicillin-sensitive *Staphylococcus aureus* (MSSA) were used. ATCC®25923™ was used for all *in vitro* experiments whereas, to allow easy strain identification, the superfolder GFP-containing strain AH1710 [44] was used for experiments in rabbit cadavers. Overnight MSSA cultures were subcultured, 2 hr and diluted in trypticase soy broth (TSB) or human synovial fluid (SynF, "discarded" from joint aspirations (approved by TJU IRB)) to $\sim 10^5$ colony forming units (CFU)/ml using a 0.5 McFarland standard (turbidity standard where A_{600} of 0.10 yields $\sim 1 \times 10^8$ CFU/ml). Inoculated surfaces were incubated under static conditions to facilitate biofilm formation. Upon harvesting, surfaces were gently washed 3X with PBS to remove nonadherent bacteria and either (i) fixed and visualized with scanning electron microscopy (SEM) or (ii) adherent bacteria suspended by 15 min sonication in 0.3% Tween 20 in PBS, followed by serial dilution, plating on 3 M™ PetriFilms™ (3 M Corp, St. Paul, MN), and digital recording. Dilutions with 20–500 CFU/film were counted and numbers expressed as CFU/ml.

2.3. Microscopy and contact angle measurements

80×80 μm areas of PEEK and PS discs were probed for surface roughness using an Asylum MFP-3D atomic force microscope (AFM, Asylum Research, Oxford Instruments) operated in tapping mode in air. Root mean square (RMS) roughness was calculated from topographic images after plane subtraction and drift correction. Four samples of each surface type were assessed. For visualization with scanning electron microscopy (SEM), surfaces with biofilms were fixed with 4% paraformaldehyde, 1 h; dehydrated with an ethanol series, air-dried overnight, sputter-coated with gold, and visualized using a Hitachi TM-1000 SEM (Hitachi High-Technologies). For each condition, at least 3 independent surfaces were assessed.

Rough contact angles were measured on dry surfaces or after pre-incubation in SynF, or TSB for 1 hr at room temperature. Perpendicular views of droplets formed with 10 μL of distilled water were recorded digitally and angles measured using two methods – (1) direct measurement of the angle of the intersection with the surface of (2) measurement of the heights and the radii of the drops, followed by calculation of the angles from their ratios.

Please cite this article as: L. J. Delaney, D. MacDonald, J. Leung et al., Ultrasound-triggered antibiotic release from PEEK clips to prevent spinal fusion infection: Initial evaluations, Acta Biomaterialia, https://doi.org/10.1016/j.actbio.2019.02.041

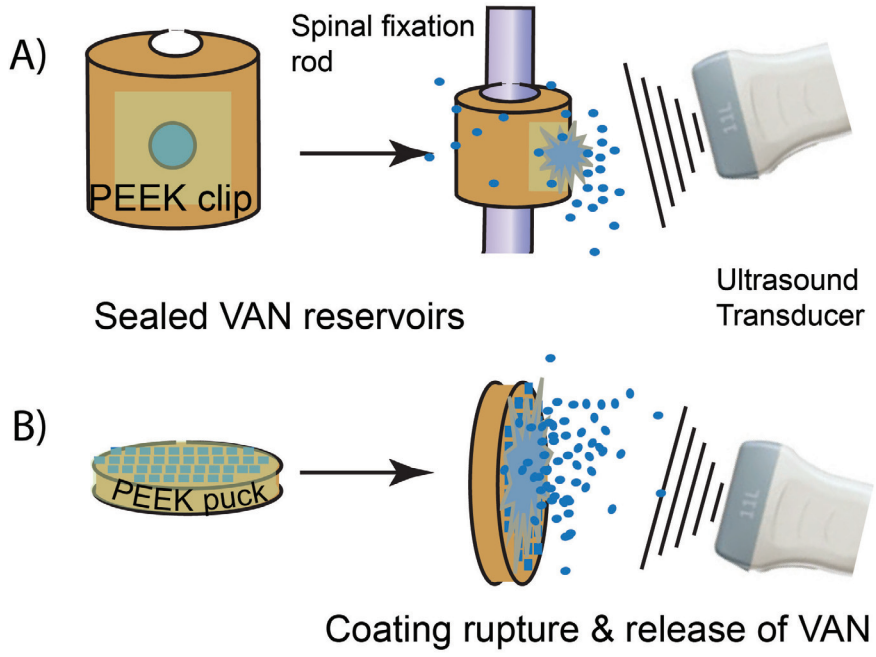

Fig. 1. Representation of loaded, sealed spinal clip (A) and porous PEEK puck (B) (elements not shown to scale). The clip (A) is shown with one-hole where the C-shaped area is for attachment to the spinal rod. The puck (B) has an array of pores. The coating on top of the reservoirs is insonated by US, causing rupture of the PLA coating to release the vancomycin (VAN).

2.4. First generation porous PEEK pucks

Additively manufactured (using the printing parameters mentioned above), porous PEEK pucks (1 cm diameter × 0.5 cm height) were loaded with 0.5 ml of a 100 mg/ml solution of VAN (50 mg; pharmaceutical grade, Athenex, Buffalo, NY) in water and frozen overnight, −20 °C, to create a solid surface for PLA coating. A subset of loaded pucks were coated with a PLA membrane by dipping the frozen puck in a solution of 1 g PLA (75–120 kDa, Resomer Select 100 DL 7E PLA, Evonik Industries, Essen, Germany) in 30 ml chloroform ($CHCl_3$, Fisher Scientific), followed by overnight air-drying at room temperature.

Coated, antibiotic-loaded pucks were submerged in 5 ml TSB containing 10^5 CFU/ml ATCC®25923™. Individual pucks were insonated by US for 10 min with a SonoScape S9 with an L742 probe (SonoScape, Shenzhen, China) in power Doppler mode at a frequency of 7.2 MHz, pulse repetition frequency of 8 kHz, and 100% acoustic output power. One and 24 hr after insonation, antibiotic release was determined by sampling 50 μL from each well, followed by spotting and drying onto a BD BBL™ blank Sensi-Disk™ (Becton Dickinson, Franklin Lakes, NJ). The disc was then placed onto a TSB agar plate containing a lawn of ATCC®25923™, and, after overnight incubation, 37 °C, the zone of inhibition due to VAN diffusion measured [45]. VAN amounts were estimated by comparison to a standard curve of VAN concentrations as well as to a commercial 30 μg VAN standard disc [9,46]. In parallel, planktonic bacterial survival was measured by plating aliquot dilutions onto 3 M™ PetriFilms™. Finally, puck-adherent ATCC®25923™ bacteria were measured at 24 hr (see 2.1). Controls included (1) coated, loaded pucks, not insonated, (2) loaded, uncoated pucks ± insonation, and (3) bacteria only ± insonation. Results were collected in triplicate and experiments repeated at least three times.

2.5. Second generation PEEK clips

Building upon our findings with the first generation PEEK pucks, we refined the design to a more clinically-relevant geometry, and continued to characterize the devices. C-shaped clips were drafted with an inner drug reservoir and designed to clip onto a standard 5.5 mm lumbar spinal fusion rod (Fig. 1), using Solidworks 2016 (Dassault Systemes, Vélizy-Villacoublay, France), and exported as a stereolithography (STL) file. These STL files were sliced and translated to G-Code, a numerical control programming language used by 3D printers for coordinates, using commercially available slicing software (Simplify3D, Cincinnati, OH). Briefly, a 0.785 cm^3 reservoir was printed into a PEEK clip using a PEEKMed filament on an Indmatec HPP 155/Gen 2 3D printer (Apium) [47]. These semi-circular clips contained either one 4 mm diameter opening (1-hole), or two 2 mm openings (2-hole). The two device designs were evaluated to compare membrane stability, as well as VAN elution time. Printed clips were evaluated for height, width, diameter, wall thickness, horizontal channel, vertical channel, and porosity using computer tomography (Scanco μCT 80, Scanco Medical, Brüttisellen, Switzerland) at 0.01 mm voxel resolution and compared to design dimensions.

To evaluate membrane stability, methylene blue (MeB), an intense dye which is widely used to visualize drug release [48–51], was used to visualize structural integrity of the membrane before and after insonation. Both the 1-hole and 2-hole clips were loaded with 120 mg of powdered MeB, or with 125 mg using a 200 mg/ml solution of MeB that was frozen to create a solid surface for coating. Loaded clips (4/group) were coated by submersion and withdrawal in a solution of (1) 50 mg/ml PLA/$CHCl_3$ for 5 times (5–50 group), (2) 50 mg/ml PLA/$CHCl_3$ for 10 times (10–50 group), or (3) 250 mg/ml PLA/$CHCl_3$ 5 times (5–250 group); all clips were dried under continuous air-flow at room temperature for 24 hr. PLA deposition was determined by weight difference before and after coating. One clip from each group was sputter coated with platinum-palladium and surface morphology determined by acquisition of 3 random images using SEM (Philips FEI XL 30 Environmental SEM (Philips, Hillsboro, OR)).

To test for release and stability, these PLA coated, MeB-loaded clips were submerged in 200 ml PBS at 37 °C with moderate shaking (90 rpm) and release was evaluated spectrophotometrically

Please cite this article as: L. J. Delaney, D. MacDonald, J. Leung et al., Ultrasound-triggered antibiotic release from PEEK clips to prevent spinal fusion infection: Initial evaluations, Acta Biomaterialia, https://doi.org/10.1016/j.actbio.2019.02.041

(λ = 600 nm; Tecan Infinite M1000, Männedorf, Switzerland) over a period of 7 days, where 1 ml was collected from the bulk liquid every 24 hr. After 7 days of incubation, clips were insonated using a SonixRP scanner equipped with an L4-9 probe (Analogic Ultrasound, Richmond, British Columbia, Canada) at a frequency of 5 MHz with a 3 MPa peak-to-peak acoustic output pressure. MeB release from the reservoir was determined as above. Results were collected in triplicate.

Burst release from uncoated MeB-loaded PEEK clips (both 1-hole and 2-hole designs) was determined while submerged in 200 ml PBS at 37 °C and shaken at 90 rpm to simulate biological fluid flow. Media was sampled and refreshed every 30 min for 10 hr and release was measured spectrophotometrically (as above). Release data was fit by linear regression to determine the diffusion coefficient, D_o, for comparison with published values. Release from the PEEK clip was modeled using the principle of Noyes-Whitney dissolution and diffusion [52–57]. Under biological conditions where constant immersion is assumed, solid drug will constantly dissolve and diffuse out of the porous PEEK clip to reach a steady state. Our model considers two routes of drug release: linear release from the drug delivery channel (N_C) and radial release from the porous cylindrical walls of the clip device (N_W). Total drug release from the clip is described by the release rate (Q_T), as shown in Eq. (1) (variables defined in Table 1).

$$\frac{dQ_T}{dt} = D_O \frac{A_{CHAN}}{M_o} \frac{(C_s - C_o)}{x} + \frac{D_o \varepsilon}{R_o * \tau * M_o} \frac{C_S * A_{CYL}}{\ln(R_i/R_o)} \quad (1)$$

VAN release from these second generation clips was evaluated *in vitro* in the same way the first generation clips were tested. Both the 1-hole and 2-hole PEEK clips were loaded with 150 μL of a 400 mg/ml solution of VAN (60 mg total) in water and frozen overnight, −20 °C, to create a solid surface for PLA coating. A subset of loaded clips were coated with a PLA membrane by dipping the frozen clip in a solution of 1 g PLA in 30 ml chloroform, followed by overnight air-drying at room temperature, as detailed for previous methods. Prepared clips were submerged in 5 ml TSB and insonated for 10 min with the same settings described previously. One and 24 hr after insonation, antibiotic release was determined by sampling 50 μL from each well, followed by spotting and drying onto a BD BBL™ disc, which was then placed onto a TSB agar plate containing a lawn of ATCC®25923™, and, after overnight incubation, 37 °C, the zone of inhibition due to VAN diffusion measured.

Table 1
Parameters used in the model and their corresponding values.

	Parameter	Description	Value
Experimental	dQ_T/dt	Release Rate	3.27%/h
	D_o	Diffusion Coefficient	7.16×10^{-8} m²/s
Solidworks	A_{CHAN}	Cross-Sectional Area of Channel	7 mm²
	A_{CYL}	Cylindrical Surface Area of Clip	339 mm²
	x	Wall Thickness	1.5 mm
	R_o	Outer Radius of Clip	6 mm
	R_i	Inner Radius of Clip	4.5 mm
	M_o	Initial Mass of Loaded Drug	120 mg
μCT	ε	Porosity	0.38
Literature	C_S	Solubility of MeB in Water	4.36×10^7 mg/m³
	τ	Tortuosity Factor	3
	C_O	Concentration of MeB in Water	0

Experimental parameters were determined through the burst release experiment, designed parameters are controlled through the design of the clip, porosity was evaluated via μCT, and literature values were found in scientific publications. [55,80]. Concentration of MeB in water is considered as zero, since the media surrounding the clip is considered an infinite sink.

VAN amounts were estimated by comparison to a standard curve of VAN concentrations as well as to a commercial 30 μg VAN standard disc.

2.6. Ex vivo evaluation of antibiotic release

US-triggered release of VAN from 1- and 2-hole PEEK clips was evaluated in a cadaveric rabbit model. Devices were loaded until filled with a slurry of 400 mg/ml VAN in water (125 μL slurry/clip = 50 mg VAN), frozen to create a solid surface for PLA coating, coated using the 5–50 protocol, and dried at room temperature for 24 hr. VAN-loaded, coated devices were sterilized by incubation in 70% ethanol (30 min) and implanted into cadaveric, mature (~6 months, 3 kg), female White New Zealand rabbits (n = 4, Covance, Princeton, NJ) under an IACUC-approved protocol. Specifically, 4 incisions were made medial to the midline of the spine; loaded, coated devices were placed in all 4 sites, and 10^4 CFU *S. aureus* AH1710 were added to 2 of the sites (Table 2). Wounds were closed with Proline 2.0 suture (Ethicon, Somerville, NJ), followed by insonation of 2 of the 4 sites for 20 min with a Logiq E9 clinical US scanner (GE Healthcare, Milwaukee, WI) equipped with a C1-6 curvilinear probe, using power Doppler imaging (1.7 MHz frequency, 6.4 kHz PRF, 100% acoustic output power) to induce cavitation and rupture of the PLA coating for VAN release (Table 2). In parallel, positive and negative bacterial controls were evaluated, where the surgical procedure was performed without PEEK devices or insonation, and *S. aureus* AH1710 added to 2 of the 4 surgical sites. All sites were incubated for 2 h, then retrieved for analysis. To confirm retrieval of GFP-labeled bacteria, sites were swabbed and the PBS-soaked swab spread onto a TSB agar plate. VAN release from the devices was quantified by zones of inhibition (see 2.3). Results were collected in duplicate for each evaluated device and condition.

2.7. Statistical analysis

All statistical testing was done using Prism 7 (GraphPad, San Diego, CA) using $\alpha = 0.05$ significance level. Error bars are displayed as standard deviation (SD). Comparison between clip design dimensions and actual device dimensions was performed using a two-tailed *t*-test. Statistically significant differences for multiple groups were determined using a one-way ANOVA with Bonferroni correction for multiple comparisons and Tukey's multiple comparison post-test when appropriate. Differences were evaluated across all groups, and also within each group for more robust analysis.

3. Results

3.1. Strain growth and biofilm formation

We first evaluated *S. aureus* ATCC®25923™ adhesion on PEEK and PS (control) surfaces to determine biofilm morphology and colonization as a function of media. On the PEEK surface at 24 hr, ATCC®25923™ appeared to be already encased in a biofilm in both

Table 2
Experimental conditions for *ex vivo* device evaluation.

Head	
Site 1 (+MSSA AH1710, −US)	Site 4 (−MSSA, −US)
Site 2 (+MSSA AH1710, +US)	Site 3 (−MSSA, +US)
Tail	

Table is arranged to depict actual device placement during experiment: middle line represents the midline/spine, MSSA (AH1710)-positive conditions were kept on the left to prevent cross contamination of surgical sites, while US-positive conditions were kept on the bottom to prevent accidental insonation of other sites.

Please cite this article as: L. J. Delaney, D. MacDonald, J. Leung et al., Ultrasound-triggered antibiotic release from PEEK clips to prevent spinal fusion infection: Initial evaluations, Acta Biomaterialia, https://doi.org/10.1016/j.actbio.2019.02.041

the ideal medium TSB (Fig. 2Aa), and after incubation in SynF (Fig. 2Ac). ATCC®25923™ colonization of PS surfaces appeared abundant in TSB (Fig. 2Ab); in SynF, the bacteria organized into three-dimensional, fibrous aggregates (Fig. 2Ad). When bacterial colonies were retrieved from the surfaces, PEEK was more abundantly colonized than PS in TSB and in SynF ($p < 0.0001$, Fig. 2B). Of interest, colonization of both PEEK and PS appeared ~4-fold lower in SynF than in TSB. Thus, while both surfaces are abundantly colonized, fibrous aggregates may influence apparent bacterial counts.

We next tested whether bacteria were able to colonize the surface in the presence of VAN. At all times and on both PS and PEEK, 10 μg/ml VAN effectively lowered numbers of adherent bacteria by 2.5–4 logs ($10^{2.5}$–10^4 decrease) when cultured in TSB (Fig. 3A and B; $p < 0.0001$ for all times when comparing 10 μg/ml VAN to 0 μg/ml VAN). VAN was less effective in SynF, achieving limited long-term reduction in CFU (Fig. 3C and D; $p < 0.0001$ for all 0 vs. 10 μg/ml VAN) except at 48 h on PS ($p = 0.0011$) and 18 and 24 h on PEEK ($p = 0.0003$ and 0.3, respectively).

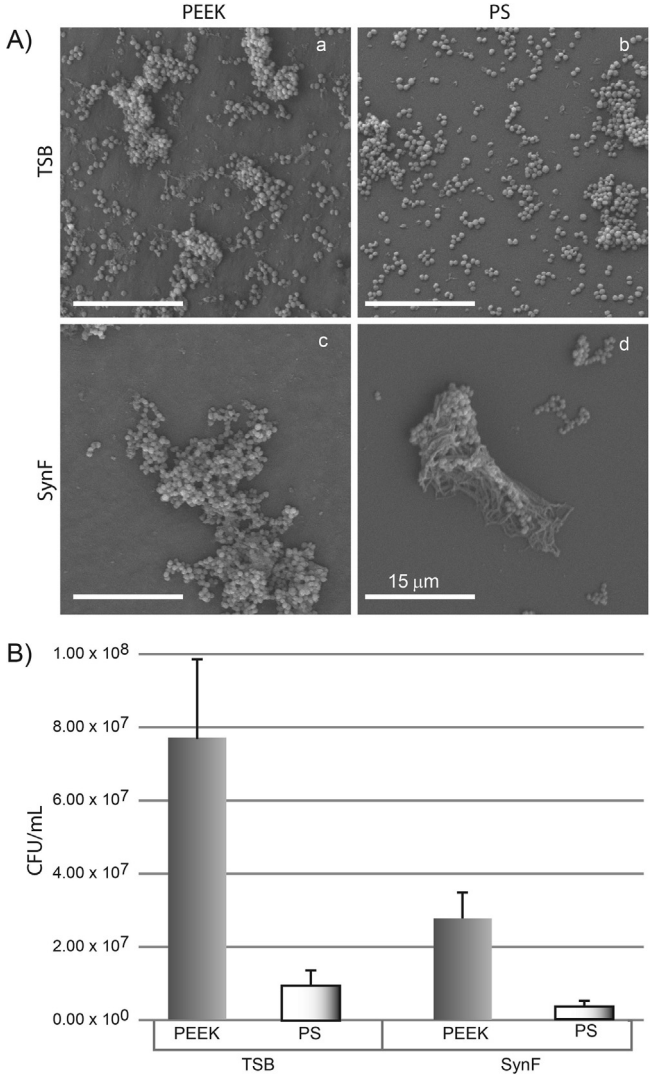

Fig. 2. Colonization of PEEK or PS in indicated media. (A) MSSA colonization of PEEK (a,c) and PS (b,d) in TSB (a,b) or SynF (c,d) is shown by SEM. Magnification: bar = 15 μm. (B) Numbers of adherent bacteria on PEEK or PS in TSB (left) or SynF (right) expressed as colony forming units (CFU)/ml. Results are average ± SD, where n = 6 in at least 3 similar, independent experiments. All values are significantly different ($p < 0.0001$).

We next tested how much VAN would be required to minimize ATCC®25923™ colonization of the surfaces. A dose of 100 μg/ml is the minimum dose for eradication of bacteria from PEEK or PS in TSB ($p < 0.008$). Large variance in bacterial counts is present at the 10 μg/ml dose in PEEK/TSB, representing inconsistent bacterial response to VAN. (Fig. 4A). A dose of 500 μg/ml is the minimum dose for eradication of bacteria from PEEK or PS in SynF ($p < 0.0001$). Significant reduction in bacterial adhesion is observed at 10 μg/ml ($p < 0.0001$, compared to 0 μg/ml) and again at 100 μg/ml ($p < 0.0001$, compared to both 0 μg/ml and 10 μg/ml) but adherent bacteria are not fully eradicated at either dose (Fig. 4B). This difference is potentially due to the aggregation and antibiotic recalcitrance previously reported [19,20].

3.2. Microscopy and contact angle measurements

As bacterial adherence is affected by surfaces properties, we characterized roughness and wettability for PEEK and PS. By SEM, 3D-printed PEEK surfaces (Fig. 5Aa) appeared rougher than PS (Fig. 5Ab), and it appeared that the PEEK surfaces had small amounts of fabrication debris. AFM analysis showed regular deep pits and topographic highs in the PEEK sample (Fig. 5Ba), whereas the PS sample showed only small variations (Fig. 5Bb). These topographic differences were more apparent in 3D views where the additive-manufactured PEEK sample (Fig. 5Ca) showed ~10X greater RMS roughness than the PS sample (Fig. 5Cb). Contact angle measurements (Table 3) indicated that the dry surfaces were less hydrophilic than those that had been pre-conditioned with TSB or SynF. However, TSB markedly changed wettability of PEEK (54° vs. 28°) but less so for PS (69° vs. 64°). Pre-coating with SynF caused both the PEEK and PS samples (contact angles 20° and 0°, respectively) to become hydrophilic.

3.3. First generation porous PEEK pucks

Having defined efficacious antibiotic amounts, we set out to develop a PLA coating that could be ruptured with US. The VAN-loaded and PLA-coated PEEK pucks were insonated with US in the presence of bathing MSSA. VAN was released due to rupture of the coating (Fig. 6) and, after 24 hr, particulates that are most likely VAN, could be visualized in the bottom of all wells holding VAN-loaded pucks, i.e., insonated coated, insonated uncoated or non-insonated uncoated. All VAN-loaded pucks, regardless of coating or insonation, caused eradication of the bathing planktonic MSSA ATCC®25923™ (data not shown). At all time points, samples taken from unloaded, uncoated, and non-insonated PEEK pucks showed no inherent antimicrobial activity compared to free growth controls ($p > 0.99$). It is worth noting that control experiments determined that insonation with US had no effect on bacterial survival ($p > 0.99$). When the pucks were examined for VAN release (Fig. 6C), a background release of VAN averaging 340 ± 168 μg was measured prior to insonation. Upon insonation (t = 0), an average of 760 ± 159 μg was measured; this release was significantly greater than the background release ($p = 0.005$). Release at 1 h (1000 ± 192 μg) was not significant compared to t = 0 ($p = 0.4$); nor was release at 24 h (2140 ± 952 μg) compared to t = 0 ($p = 0.08$) or t = 1 h ($p = 0.2$). Using average cumulative release, VAN release increased markedly with time ($p = 0.0002$). Immediately following insonation, an average cumulative release of 1.1 ± 0.3 mg was measured ($p = 0.0004$ compared to before US); at 1 hr, average cumulative release was 2.1 ± 0.3 mg ($p = 0.0003$ compared to t = 0), and at 24 h, total release was 4 ± 1 mg out of a total of ~50 mg loaded into each puck ($p = 0.001$ compared to before US, $p = 0.003$ compared to t = 0, and $p = 0.01$ compared to t = 1).

Please cite this article as: L. J. Delaney, D. MacDonald, J. Leung et al., Ultrasound-triggered antibiotic release from PEEK clips to prevent spinal fusion infection: Initial evaluations, Acta Biomaterialia, https://doi.org/10.1016/j.actbio.2019.02.041

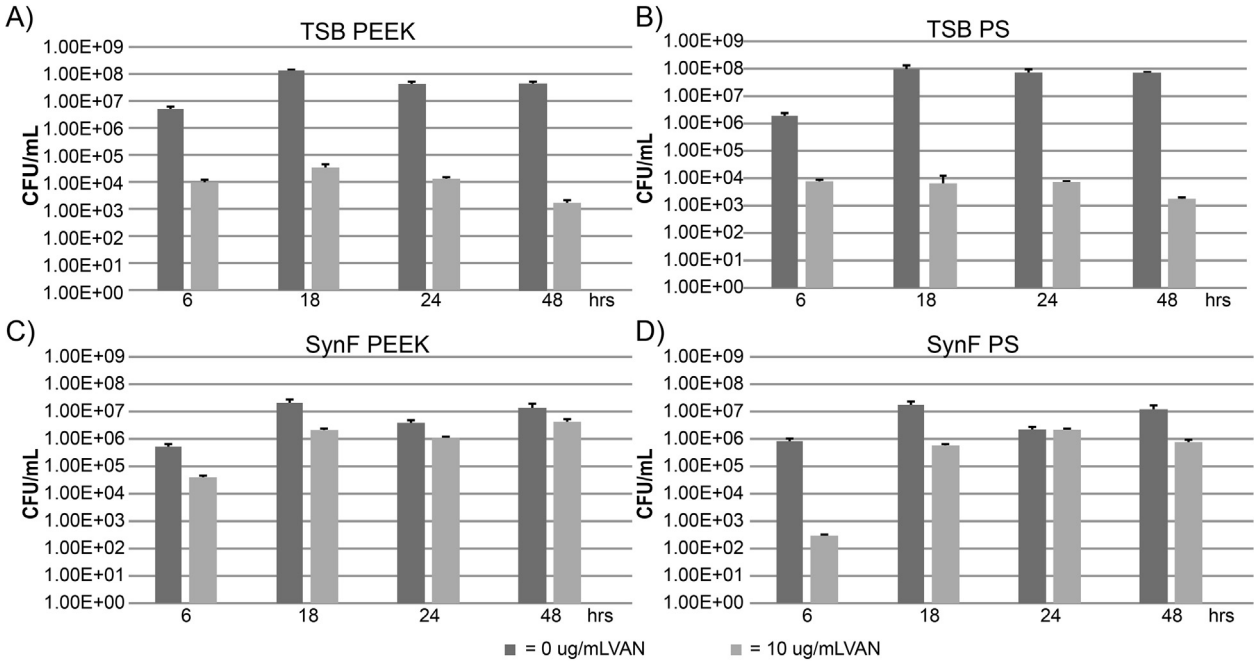

Fig. 3. MSSA colonization of PEEK or PS in TSB or SynF over time. Graphs are MSSA incubated in TSB (A and B) or SynF (C and D) on PEEK (A and C) or PS (B and D). Each graph shows colonization on control compared to that in the presence of 10 μg/ml VAN. Note that CFU/ml are plotted on a log scale. Numbers of bacteria are represented as CFU/ml and represent average ± SD ($n > 6$, with at least 3 similar, independent repeats). For SynF on PS at 18 and 24 h, p values for 0 vs. 10 μg/ml VAN were $p = 0.0003$ and 0.3, respectively. For SynF on PEEK, 0 vs. 10 μg/ml VAN at 48 hr achieved a significance of $p = 0.001$. All other comparisons were significantly different at $p < 0.0001$.

3.4. Second generation PEEK clips

After successfully releasing sufficient quantities of VAN to eradicate all bacteria, and confirming the feasibility of the US-triggered release in a basic puck design, we investigated whether we could translate this US-mediated release using a reservoir that would fit onto spinal rods. Two C-shaped PEEK clip designs, a 1-hole clip and a 2-hole clip, were manufactured and characterized. Dimensional accuracy of the PEEK clip prototypes was verified with μCT measurements, with no significant difference found between designed and measured dimensions ($p > 0.9$, data not shown).

Evaluating the coating process for both the 1-hole and 2- hole clip designs, PLA deposition on the clips appeared successful, but was variable for both the 5–50 and the 10–50 techniques (on average 47 ± 56 mg of PLA for the 5–50 technique vs. 87 ± 105 mg for the 10–50 technique; $p = 0.005$). The 5–250 coatings were more consistent (average PLA deposit = 214 ± 57 mg) and deposited significantly greater amounts of PLA than the other techniques ($p < 0.0001$). These findings are consistent with the coating morphology observed via SEM imaging (Fig. 7A). The coatings observed with the 5–50 (Fig. 7Ab) and 10–50 (Fig. 7Ac) techniques were heterogeneous, with porosity still apparent; the 5–250 technique (Fig. 7Ad) completely covered the PEEK surface and its pores. Quantitatively for both the 1-hole and 2-hole clip designs, the 5–50 coating showed the greatest innate release over time (24 ± 3%), followed by the 10–50 coating (17 ± 7%), as shown in Fig. 7B. The 5–250 coating retained the MeB for the 7 days of the trial (0.6 ± 0.6%, $p < 0.01$).

When the clip membranes were ruptured by US insonation, small gas bubbles were seen escaping from the reservoir inside the PEEK clips and MeB was observed streaming from the reservoir into the surrounding PBS (Fig. 7C, with the 1-hole clip design as a visual example); however, concentrations were not measured post-insonation, due to loss of fluid. While the 5–250 coating allowed more stable retention of material, the 5–50 coating showed more reproducible rupture in both the one-hole and two-hole designs and was used in the *in vitro* and *ex vivo* VAN release experiments.

Evaluation of burst release from the one-hole PEEK clips revealed that release was linear, and aligned with the model (cf., Eq. (1)), with a rate of 3.3% per hour over the first three hours of submersion ($r^2 > 0.99$, data not shown); similar rates were observed for the two-hole PEEK clips. Using published values for spherical pore tortuosity factor and MeB solubility, the diffusion coefficient of MeB was calculated as 7.2×10^{-8} m^2/s [55,57–59]. Beyond 8 hr, the cumulative release of MeB asymptotically reached 98%, signifying the complete emptying of the reservoir contents into the submersion medium. We also evaluated both the one-hole and two-hole clip designs for VAN release from the uncoated clips under static conditions. There was significantly greater total VAN release from the one-hole design (772 ± 66 μg) than from the two-hole clip (512 ± 115 μg, $p = 0.01$).

When the clips were examined for US-triggered VAN release (Fig. 8), the PLA membrane on the one-hole design appeared to be more stable and responsive to insonation than with the two-hole design. Background release for the coated, uninsonated one-hole clip was 5 ± 6 μg after submersion for 1 h, while the two-hole clip released 20 ± 5 μg over the same time ($p = 0.01$). This was also the case at 24 h, where the two-hole clips released 453 ± 3 μg VAN, while the one-hole design released significantly less VAN (169 ± 3 μg, $p < 0.0001$). Additionally, the two-hole clip showed no significant difference between the insonated and uninsonated samples (Fig. 8B) at any of the time points ($p > 0.8$). Conversely, the one-hole clip design showed that VAN release increased markedly with time ($p < 0.0001$, Fig. 8A). One hour following insonation, an average release of 74.7 ± 0.6 μg was measured ($p = 0.0002$ compared to uninsonated). After 24 h, the total cumulative release from the insonated one-hole clips was 527 ± 32 μg ($p = 0.0002$ compared to uninsonated). Comparatively, there was no significant difference in total US-triggered VAN release between the one-hole design and the two-hole design (486 ± 107 μg, $p = 0.3$). Therefore, we continued to evaluate

Please cite this article as: L. J. Delaney, D. MacDonald, J. Leung et al., Ultrasound-triggered antibiotic release from PEEK clips to prevent spinal fusion infection: Initial evaluations, Acta Biomaterialia, https://doi.org/10.1016/j.actbio.2019.02.041

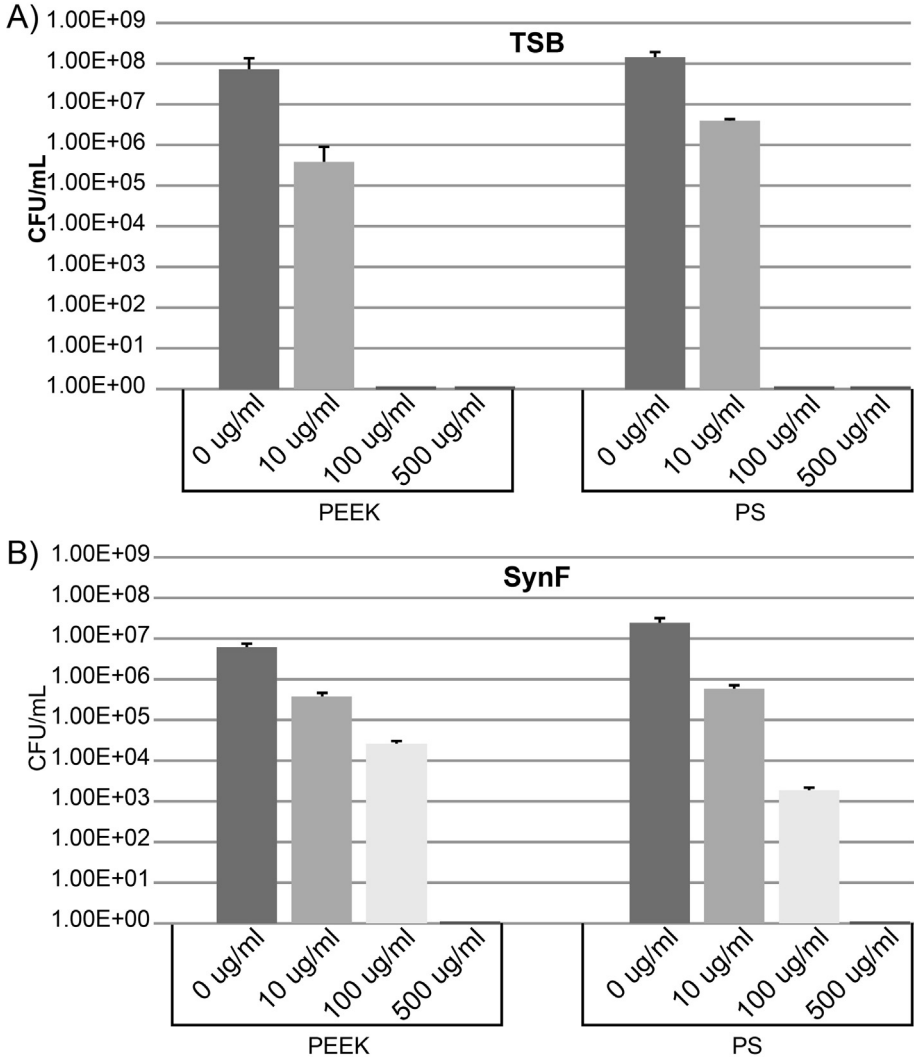

Fig. 4. Effects of different doses of VAN on MSSA colonization. Adherent MSSA were counted after incubation in the indicated amounts of VAN and expressed as CFU/ml. Note log scale. Values shown are average ± SD (n = 6, with at least 3 independent repeats). For TSB on PEEK, 0 vs. 10 μg/ml VAN was p = 0.02, 0 vs. 100 μg/ml VAN and 0 vs. 500 μg/ml VAN were both p = 0.008. For TSB on PS, all comparisons except 100 vs. 500 μg/ml VAN were p < 0.0001. For TSB on PEEK and PS, 100 vs. 500 μg/ml VAN was p > 0.99. For SynF on PEEK and PS, all comparisons were p < 0.0001.

both the one-hole and two-hole clip designs in the *ex vivo* experiments.

3.5. Ex vivo evaluation of antibiotic release

Based on our successful *in vitro* evaluation of these clinically-relevant prophylactic PEEK clips, we studied the characteristics of US-mediated VAN release and elution in an *ex vivo* spine model. Representative images of device implantation and insonation in a cadaveric, female, New Zealand white rabbit are shown in Fig. 9. Negative controls indicated no surgical site contamination, and positive controls confirmed that the GFP-expressing MSSA AH1710 grew in the wound environment.

In terms of bacterial recovery (data not shown), retrieved bacteria expressed GFP, consistent with recovery of *S. aureus* AH1710. Because swabbing is not quantitative, antimicrobial efficacy could not be enumerated, but numbers of bacteria in sites that had had VAN release by US appeared less abundant than those with no facilitated release. VAN release was dependent on the design. Specifically, using the porous puck, roughly 50% (by weight) of the encapsulated VAN was released by insonation *in vitro*, compared with no VAN release from the non-insonated pucks. When we moved to *ex vivo* conditions, both the 1-hole and 2-hole clips, showed time-dependent VAN release. At 48 hr, there was significantly greater VAN release from the insonated clips compared to the uninsonated clips for both designs ($p < 0.04$; Fig. 9D and E). There was significantly greater US-triggered total VAN release from the 1-hole clip design (7420 ± 2992 μg) than from the 2-hole design (3500 ± 954 μg, $p < 0.0001$). Thus, the 1-hole clip design showed a greater release than the 2-hole design, suggesting that the larger hole may allow the greatest drug release.

4. Discussion

Despite the placement of up to 2 g of VAN during spinal fusion surgeries, bacteria remain, propagate, and establish an infection in up to 5.2% of cases [13,14]. These antibiotics are thought to be depleted by the presence of aseptic drains, commonly removed at 2 or 3 days. We reasoned that release of a second prophylactic dose of antibiotics in the post-surgical period (2–7 days) could eradicate bacteria that escaped the initial prophylaxis. With that in mind, we designed a system for antibiotic release within the spine that would achieve a slow release over several days, followed

Please cite this article as: L. J. Delaney, D. MacDonald, J. Leung et al., Ultrasound-triggered antibiotic release from PEEK clips to prevent spinal fusion infection: Initial evaluations, Acta Biomaterialia, https://doi.org/10.1016/j.actbio.2019.02.041

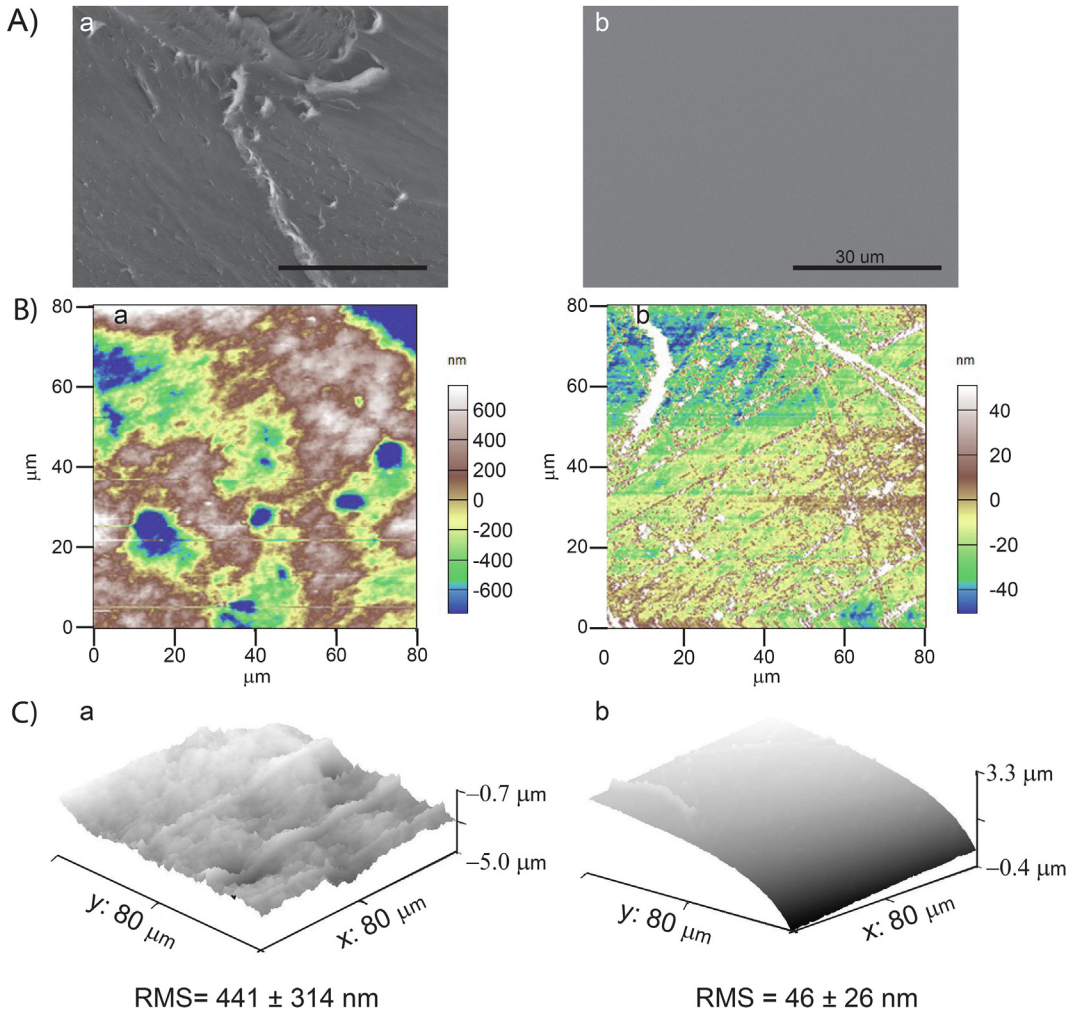

Fig. 5. Surface assessment of PEEK and PS. A) SEM imaging of PEEK (a) and PS (b) at 3.5kX magnification. Magnification: bar = 30 µm. B) Topographical map of roughness, as measured by AFM, of PEEK (a) and PS (b). The roughness scale is shown to the right of each of the plots. C) Three dimensional representation of PEEK (a) and PS (b) topography. Measured root mean square (RMS) roughness is shown for each sample (RMS ± SD).

Table 3
Contact angles.

	PEEK	PS
Dry	54 ± 5	69 ± 13
TSB	28 ± 8	64 ± 5
SynF	20 ± 3	0 ± 0

Contact angles in degrees, as a function of pre-conditioning the indicated surfaces with TSB or SynF (n = 6), based on average of the arctan of the ratio of height to radius.

by a bolus release of antibiotics triggered by US-induced rupture of the PLA membrane. VAN release was visibly achieved from all three device designs. We found that PLA coating of the PEEK devices is susceptible to US disruption both *in vitro* and within tissue *ex vivo*, with up to 7.4 mg of VAN delivered within 48 hr. Our result was a viable prototype (i.e., the 1-hole clip) for US-mediated localized prophylactic delivery to the spinal surgical site.

The impetus for the development of these antibiotic-releasing devices was based on two observations. The establishment of infection peri-surgically, even with prophylaxis, [13,14] suggested that either the organism was not sensitive to VAN or that the VAN-sensitive organism had escaped due to acquisition of a "persister" phenotype. To address the first concern, our device was designed so that antibiotics with different spectra of activity could be used singly or combined, allowing for additional coverage. In the second case, because of the presence of persisters [60], even large doses of VAN may be unable to sterilize a site. Fortunately, even with our initial slow release, the pressure to remain in the persistent phenotype will be markedly reduced over the first several days and the bacteria will tend to return to a more proliferative phenotype that is again susceptible to antibiotics [60]. Thus, we reasoned that a treatment followed by a pause, followed by a second treatment would significantly decrease contaminating bacteria by reducing numbers of persisters.

Persisters are known to be part of biofilms. We and others have previously shown that SynF and blood cause aggregation of MSSA and MRSA into floating biofilms and this affects metabolism and antibiotic sensitivity [18–20]. In our experiments, MSSA preferentially colonize the additive-manufactured PEEK surfaces even though the control PS surfaces showed similar hydrophilicity after conditioning with SynF or TSB. These small differences in numbers were magnified in the presence of VAN, as surfaces in SynF required 500 µg/ml of VAN vs. 100 µg/ml of VAN in TSB, suggesting that persister formation may become even more important in physiological fluid. Based on these reports and the data shown in

Please cite this article as: L. J. Delaney, D. MacDonald, J. Leung et al., Ultrasound-triggered antibiotic release from PEEK clips to prevent spinal fusion infection: Initial evaluations, Acta Biomaterialia, https://doi.org/10.1016/j.actbio.2019.02.041

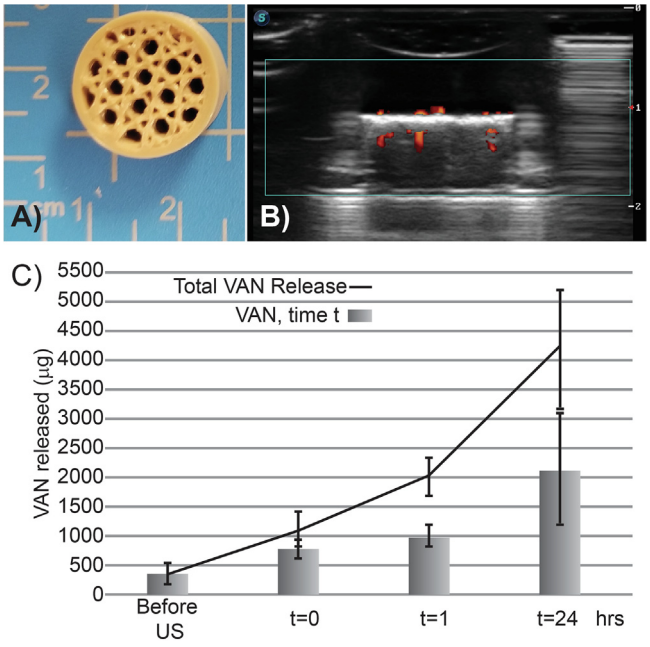

Fig. 6. Porous PEEK VAN reservoir for US release. A) Image of unloaded, 3D printed, porous PEEK disc. B) Image of *in vitro* US-triggered VAN release from the PEEK spacers. Blue box represents power Doppler imaging, focused on the spacer device. Red areas are areas of increased streaming characteristic of a ruptured coating. C) Summary of *in vitro* VAN release experiments. Values are from two independent pucks sampled three times at each point. Histogram represents progressive VAN release (not cumulative) at each time point; the line represents cumulative VAN release from the time of immersion where all VAN amounts are expressed in μg. For progressive release, the only two significant comparisons were before US vs. t = 0 ($p = 0.005$) and before US vs. t = 24 ($p = 0.03$); t = 0 vs. t = 24 was trending toward significance ($p = 0.08$). For cumulative release, all comparisons were significant ($p < 0.01$, exact values given in text).

the present study, we strongly support the use of true, protein-laden physiological fluid for measuring efficacy of antimicrobial systems. Importantly, the >100 μg amounts needed to decrease bacterial adhesion emphasize the limited utility of systems that achieve "above MIC" amounts (MIC of VAN for sensitive *S. aureus* is <2 μg/ml [61]) to decrease biofilm amounts *in vivo*. Importantly, the >100–500 μg/ml levels eluted from our devices are sufficient for eradication of MSSA biofilms, even those containing persisters.

Fortunately, it has been shown that US sensitizes adherent bacteria to antibiotics [21–23], so we do not anticipate that bacterial colonization of the clip would occur during the time course of the prophylaxis (0–7 d). Like any other implant, however, the surface of the clip, which is small compared to the metal hardware, could conceivably serve as an additional surface for bacterial colonization. We do hypothesize that the interior reservoir, due to small amounts of unescaped VAN and no flow, would still be relatively inhospitable to bacteria – this will have to be determined in animal experiments.

An additional concern is the fostering of resistant organisms. Because of the high, temporally-limited, levels of antibiotics, it is unlikely that prolonged selective pressure will exist on the resident contaminants, allowing them to acquire resistance and overgrow the suppressed population of bacteria. We specifically designed this device for an US-mediated bolus release to minimize this pressure. On the other hand, though when the antibiotic amounts are large, concerns about biocompatibility arise. Based on our previous data, we would expect the levels of VAN that are released from the devices to fall within the acceptable range (<4 mg/24 h) [62].

Based on the above discussion, we had clear design parameters that needed to be satisfied, i.e., a reservoir that could hold enough antibiotic for bolus release, a membrane that could be ruptured with US, and facilitated release of the antibiotic with insonation. The porous PEEK pucks tested initially had sufficient porosity to immobilize the large amounts of VAN required for effective eradication of MSSA. Once the PLA coating was ruptured by insonation, particulate VAN (and perhaps PLA debris) was present both in the puck and surrounding it. We suggest that the solubility of VAN was exceeded in our elution volume and thus, much of the VAN remained within the PEEK pucks. This situation would be different under the fluid flow characteristic of biological systems [63]. When the pucks were examined for VAN release, all pucks showed background release of VAN consistent with levels that would be considered antimicrobial. Based on our findings in these experiments, more tuning of the coating process is necessary to improve consistency of innate and US-triggered VAN release.

In many of the characterizations, we used the widely-accepted MeB as a model drug. This was especially important with VAN, whose spectrophotometric determination is hampered by a small extinction coefficient ($E^{1\%} = 40$ (280 nm, in H_2O, VAN) [64] vs. $E^{10\mu M} = 30580$ (600 nm in H_2O, MeB) [65]). Depending on experimental conditions, diffusion of MeB has been reported in the range of 5.5×10^{-8} m^2/s to 0.5×10^{-9} m^2/s [66–68]. Therefore, taken with our use of a shaker plate and 37 °C submersion bath to better simulate sink conditions experienced *in vivo*, our calculated value for MeB diffusion from our device agrees with published values, and validates our model of release from our PEEK clip devices.

Burst release tests demonstrated that 98% of the MeB loaded into an uncoated PEEK reservoir was released at 10 h of submersion. In contrast, even at 48 h, VAN elution was only ~7.4 mg of the possible 50 mg (~15% of the total). Again, we suggest that these differences are due to solubility and the fact that that the VAN experiments were designed to test elution in ~5–10 ml, which is characteristic of post-surgical wound fluid (CKK, personal communication). Work in living animals will be required to hone antibiotic loading and release to allow complete bolus release. In addition, studies are being conducted to determine the optimal PLA coating thickness, as we found that the membrane thickness and susceptibility to US-triggered rupture is highly tunable by varying the concentration of PLA in the solution as well as the number of coatings applied to the clip [69,70].

This study uses targeted US to mediate bulk drug release from within a spinal hardware adjunct, and is one of only a handful of studies investigating US-mediated bulk drug release. Previously, Miyazaki et al. demonstrated US-facilitated release of insulin from a polymeric implant placed subcutaneously in diabetic rats [71]. Animals receiving insonation at the implant site exhibited immediate decreases in blood glucose levels, signaling US-mediated release of insulin [71]. Additionally, Kost et al. showed the tunable effect of US pressure waves on degradation of polymers and the release rate of molecules incorporated within these polymers [72,73]. Otherwise, the majority of US-mediated drug delivery is centered around the use of hydrogels, liposomes, and microbubbles for targeted delivery [74–79].

Study limitations include a limited sample size *in vitro* and *ex vivo*, lack of fluid flow during the VAN elution experiments resulting in saturated solutions of VAN, as well as the variability in applying and determining coating thicknesses. Finally, complete independence between sites in the *ex vivo* model was assumed but cannot be guaranteed.

The ultimate translational development of the device that we have described will provide an important tool to spine surgeons in their attempts to minimize the risk of infection. Currently, prophylaxis is dependent on placement of VAN during surgical closure; additional prophylaxis is not used as it requires injection and increased chances of infection. With the possibility of a wider

Please cite this article as: L. J. Delaney, D. MacDonald, J. Leung et al., Ultrasound-triggered antibiotic release from PEEK clips to prevent spinal fusion infection: Initial evaluations, Acta Biomaterialia, https://doi.org/10.1016/j.actbio.2019.02.041

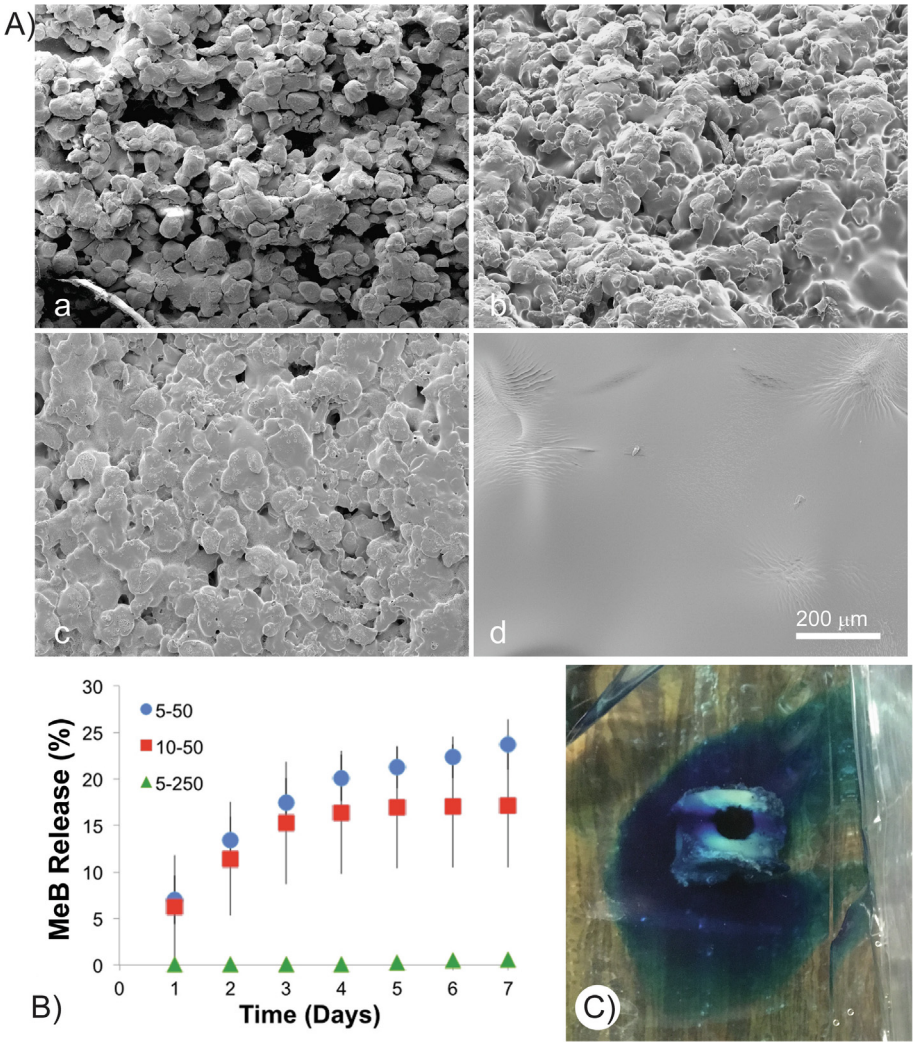

Fig. 7. PLA coating and release from porous PEEK VAN reservoir A) SEM images of PEEK spacer surfaces, magnification 120×. Magnification: bar = 200 μm. Aa) Uncoated PEEK spacer showing porous material. Ab) PEEK spacer coated using 5–50 technique showing partially coated surface. Ac) PEEK spacer coated using 10–50 technique showing partially coated surface, but more so than the 5–50 surface. Ad) PEEK spacer coated using 5–250 technique showing a completely coated, smooth surface. B) Innate MeB release from the three coating techniques. C) Representative image of increased MeB release post-insonation.

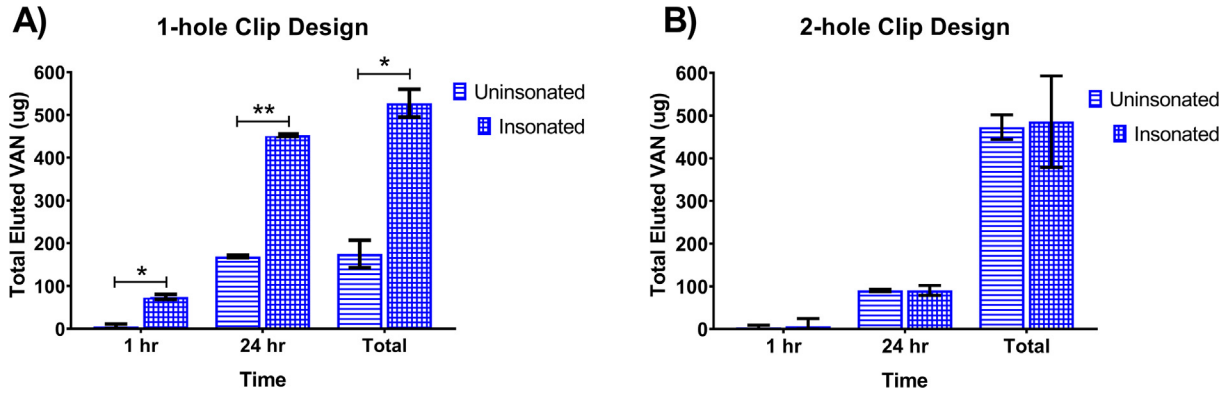

Fig. 8. *In vitro* characterization of VAN release from 1-hole and 2-hole PEEK clip designs, represented as average ± SD, values are from three independent clips sampled twice at each point. A) Elution of VAN from the 1-hole clip, *p = 0.0002, **p < 0.0001. B) Elution of VAN from the 2-hole clip.

choice for antibiotics, i.e., Gram-positive and Gram-negative targets, prophylaxis can be initiated by the VAN placement and completed by the non-invasive release from the spinal clip. Thus, by harnessing non-invasive US cavitation to effectively deliver high levels of antibiotics, we anticipate that spinal infection rates will be able to be markedly decreased.

Please cite this article as: L. J. Delaney, D. MacDonald, J. Leung et al., Ultrasound-triggered antibiotic release from PEEK clips to prevent spinal fusion infection: Initial evaluations, Acta Biomaterialia, https://doi.org/10.1016/j.actbio.2019.02.041

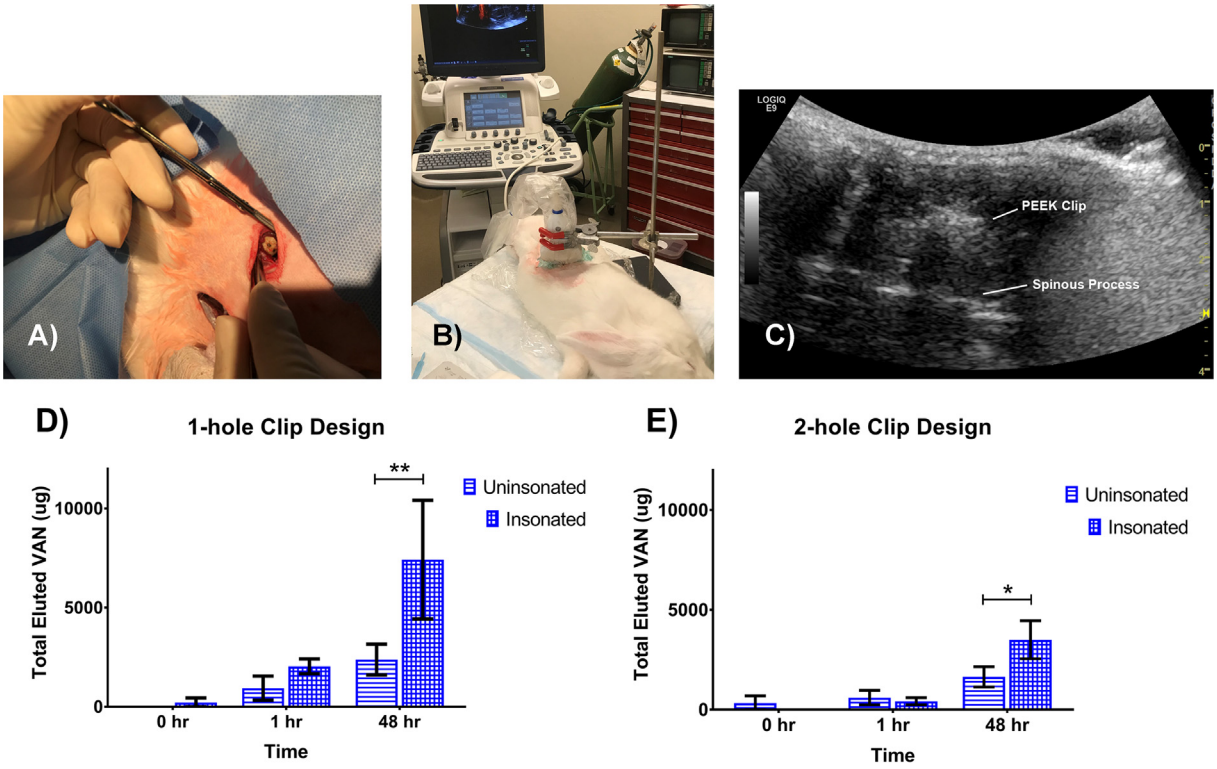

Fig. 9. Representative images of cadaveric device implantation and insonation. A) Surgical sites with implanted VAN-loaded, PLA-coated PEEK spacers. B) Insonation of closed surgical sites. C) US image of drug delivery vessel and neighboring vertebrae within surgical site. D) Elution of VAN from the 1-hole clip, represented as average ± SD, values are from two independent clips sampled three times at each point, $^{**}p < 0.0001$. E) Elution of VAN from the 2-hole clip, represented as average ± SD, values are from two independent clips sampled three times at each point, $^{*}p = 0.03$.

5. Conclusions

Existing methods for preventing peri-operative infection after spinal fusion surgery are only partially successful. To combat this clinical problem, we have designed an US-activated drug release system that can release combinations of prophylactic antibiotics to aggressively combat post-surgical bacterial survival, while avoiding the problems of controlled elution systems. Ultimately, a combination of antibiotics that target both Gram-positive and Gram-negative bacteria would be loaded into the reservoir for a broad approach to eradicating contaminating bacteria and preventing infection.

Acknowledgements

The authors thank Priscilla Machado and Catherine Gurr from Thomas Jefferson University, Cemile Basgul and Anthony Law from Drexel University, Matthew Brukman from the University of Pennsylvania, and the Drexel University Centralized Research Facility Materials Characterization Lab for their contributions. Additionally, we thank GE Healthcare for equipment support and Dr. Alexander Horswill (University of Colorado) for *S. aureus* AH1710. This work was performed in part at the University of Pennsylvania's Singh Center for Nanotechnology, an NNCI member supported by National Science Foundation (NSF) Grant ECCS-1542153. Research reported in this publication was supported by the National Institutes of Health (NIH) under award numbers R01 AR069119, F32 AR072491, and RO1 AR072513. The content is solely the responsibility of the authors and does not necessarily represent the official views of the National Institutes of Health.

Disclosures

Lauren J. Delaney, Alex M. Sevit, Keith Fitzgerald, Daniel W. MacDonald, Neil Patel, and Jay Leung have no disclosures to report. John R. Eisenbrey reports disclosures with GE Healthcare, Lantheus Medical Imaging, and GlaxoSmithKline; Flemming Forsberg with GE Healthcare and Lantheus Medical Imaging; Christopher K. Kepler with Inion, Pfizer, Medtronic, and RTI; Steven M. Kurtz with Exponent, Celanese, Ceramtec, Ferring Pharmaceuticals, Invibio, Simplify Medical, Stelkast, Stryker, Wright Medical Technology, and Zimmer Biomet; and Noreen J. Hickok with IBX, Irrisept, and SterileBits. None of these entities funded this work.

References

[1] S.M. Kurtz, E. Lau, J. Schmier, K.L. Ong, K. Zhao, J. Parvizi, Infection burden for hip and knee arthroplasty in the United States, J. Arthroplasty 23 (7) (2008) 984–991.
[2] S.M. Kurtz, E. Lau, K.L. Ong, L. Carreon, H. Watson, T. Albert, S. Glassman, Infection risk for primary and revision instrumented lumbar spine fusion in the Medicare population, J. Neurosurg. Spine 17 (4) (2012) 342–347.
[3] K.J. Bozic, E. Lau, S. Kurtz, K. Ong, H. Rubash, T.P. Vail, D.J. Berry, Patient-related risk factors for periprosthetic joint infection and postoperative mortality following total hip arthroplasty in Medicare patients, J. Bone Joint Surg. Am. 94 (9) (2012) 794–800.
[4] J.W. Costerton, P.S. Stewart, E.P. Greenberg, Bacterial biofilms: a common cause of persistent infections, Science 284 (5418) (1999) 1318–1322.
[5] F. Furno, K.S. Morley, B. Wong, B.L. Sharp, P.L. Arnold, S.M. Howdle, R. Bayston, P.D. Brown, P.D. Winship, H.J. Reid, Silver nanoparticles and polymeric medical devices: a new approach to prevention of infection?, J Antimicrob. Chemotherapy 54 (6) (2004) 1019–1024.
[6] A. Reznickova, Z. Novotna, O. Kvitek, Z. Kolska, V. Svorcik, Gold, silver and carbon nanoparticles grafted on activated polymers for biomedical applications, J. Nanosci. Nanotechnol. 15 (12) (2015) 10053–10073.

Please cite this article as: L. J. Delaney, D. MacDonald, J. Leung et al., Ultrasound-triggered antibiotic release from PEEK clips to prevent spinal fusion infection: Initial evaluations, Acta Biomaterialia, https://doi.org/10.1016/j.actbio.2019.02.041

[7] M.C. Lawson, K.C. Hoth, C.A. Deforest, C.N. Bowman, K.S. Anseth, Inhibition of Staphylococcus epidermidis biofilms using polymerizable vancomycin derivatives, Clin. Orthop. Relat. Res. 468 (8) (2010) 2081–2091.
[8] C. Ketonis, S. Barr, C.S. Adams, I.M. Shapiro, J. Parvizi, N.J. Hickok, Vancomycin bonded to bone grafts prevents bacterial colonization, Antimicrob. Agents Chemother. 55 (2) (2011) 487–494.
[9] V. Antoci Jr., C.S. Adams, J. Parvizi, H.M. Davidson, R.J. Composto, T.A. Freeman, E. Wickstrom, P. Ducheyne, D. Jungkind, I.M. Shapiro, N.J. Hickok, The inhibition of Staphylococcus epidermidis biofilm formation by vancomycin-modified titanium alloy and implications for the treatment of periprosthetic infection, Biomaterials 29 (35) (2008) 4684–4690.
[10] G.A. Ter Boo, D. Arens, W.J. Metsemakers, S. Zeiter, R.G. Richards, D.W. Grijpma, D. Eglin, T.F. Moriarty, Injectable gentamicin-loaded thermo-responsive hyaluronic acid derivative prevents infection in a rabbit model, Acta Biomaterialia 43 (2016) 185–194.
[11] H. van de Belt, D. Neut, W. Schenk, J.R. van Horn, H.C. van der Mei, H.J. Busscher, Infection of orthopedic implants and the use of antibiotic-loaded bone cements, A review, Acta Orthop. Scand. 72 (6) (2001) 557–571.
[12] V.J. Suhardi, D.A. Bichara, S. Kwok, A.A. Freiberg, H. Rubash, H. Malchau, S.H. Yun, O.K. Muratoglu, E. Oral, A fully functional drug-eluting joint implant, Nat. Biomed. Eng. 1 (2017).
[13] K.R. O'Neill, J.G. Smith, A.M. Abtahi, K.R. Archer, D.M. Spengler, M.J. McGirt, C.J. Devin, Reduced surgical site infections in patients undergoing posterior spinal stabilization of traumatic injuries using vancomycin powder, Spine J. 11 (7) (2011) 641–646.
[14] G.M. Ghobrial, V. Thakkar, E. Andrews, M. Lang, A. Chitale, M.E. Oppenlander, C.M. Maulucci, A.D. Sharan, J. Heller, J.S. Harrop, J. Jallo, S. Prasad, Intraoperative vancomycin use in spinal surgery: single institution experience and microbial trends, Spine 39 (7) (2014) 550–555.
[15] R.A. Brady, J.G. Leid, J.H. Calhoun, J.W. Costerton, M.E. Shirtliff, Osteomyelitis and the role of biofilms in chronic infection, FEMS Immunol. Med. Microbiol. 52 (1) (2008) 13–22.
[16] S.M. Kurtz, J.N. Devine, PEEK biomaterials in trauma, orthopedic, and spinal implants, Biomaterials 28 (32) (2007) 4845–4869.
[17] I. Collins, J. Wilson-MacDonald, G. Chami, W. Burgoyne, P. Vinayakam, T. Berendt, J. Fairbank, The diagnosis and management of infection following instrumented spinal fusion, Eur. Spine J. 17 (3) (2008) 445–450.
[18] H.A. Crosby, J. Kwiecinski, A.R. Horswill, Staphylococcus aureus aggregation and coagulation mechanisms, and their function in host-pathogen interactions, Adv. Appl. Microbiol. 96 (2016) 1–41.
[19] S. Dastgheyb, J. Parvizi, I.M. Shapiro, N.J. Hickok, M. Otto, Effect of biofilms on recalcitrance of staphylococcal joint infection to antibiotic treatment, J. Infectious Diseases 211 (4) (2015) 641–650.
[20] S.S. Dastgheyb, S. Hammoud, C. Ketonis, A.Y. Liu, K. Fitzgerald, J. Parvizi, J. Purtill, M. Ciccotti, I.M. Shapiro, M. Otto, N.J. Hickok, Staphylococcal persistence due to biofilm formation in synovial fluid containing prophylactic cefazolin, Antimicrob. Agents Chemotherapy 59 (4) (2015) 2122–2128.
[21] D. Harpaz, Ultrasound enhancement of thrombolytic therapy: observations and mechanisms, Int. J. Cardiovasc. Intervent 3 (2) (2000) 81–89.
[22] Y. Dong, J. Li, P. Li, J. Yu, Ultrasound microbubbles enhance the activity of vancomycin against staphylococcus epidermidis biofilms in vivo, J. Ultrasound Med. 37 (6) (2018) 1379–1387.
[23] J. Hu, N. Zhang Jr., L. Li, N. Zhang Sr., Y. Ma, C. Zhao, Q. Wu, Y. Li, N. He, X. Wang, The synergistic bactericidal effect of vancomycin on UTMD treated biofilm involves damage to bacterial cells and enhancement of metabolic activities, Science 8 (1) (2018) 192.
[24] Y. Zhang, J. Yu, H.N. Bomba, Y. Zhu, Z. Gu, Mechanical force-triggered drug delivery, Chem. Rev. 116 (19) (2016) 12536–12563.
[25] S.R. Sirsi, M.A. Borden, State-of-the-art materials for ultrasound-triggered drug delivery, Adv. Drug Deliv. Rev. 72 (2014) 3–14.
[26] R. Tanbour, A.M. Martins, W.G. Pitt, G.A. Husseini, Drug delivery systems based on polymeric micelles and ultrasound: a review, Curr. Pharm. Design 22 (19) (2016) 2796–2807.
[27] J.R. Eisenbrey, O.M. Burstein, R. Kambhampati, F. Forsberg, J.B. Liu, M.A. Wheatley, Development and optimization of a doxorubicin loaded poly(lactic acid) contrast agent for ultrasound directed drug delivery, J. Controlled Release 143 (1) (2010) 38–44.
[28] M.J. Shortencarier, P.A. Dayton, S.H. Bloch, P.A. Schumann, T.O. Matsunaga, K. W. Ferrara, A method for radiation-force localized drug delivery using gas-filled lipospheres, IEEE Trans. Ultrason. Ferroelectr. Freq. Control 51 (7) (2004) 822–831.
[29] S. Zhao, M. Borden, S.H. Bloch, D. Kruse, K.W. Ferrara, P.A. Dayton, Radiation-force assisted targeting facilitates ultrasonic molecular imaging, Mol. Imag. 3 (3) (2004) 135–148.
[30] M. Postema, A. van Wamel, C.T. Lancee, N. de Jong, Ultrasound-induced encapsulated microbubble phenomena, Ultrasound Med. Biol. 30 (6) (2004) 827–840.
[31] M. Postema, A. van Wamel, F.J. ten Cate, N. de Jong, High-speed photography during ultrasound illustrates potential therapeutic applications of microbubbles, Med. Phys. 32 (12) (2005) 3707–3711.
[32] C.M. Newman, T. Bettinger, Gene therapy progress and prospects: ultrasound for gene transfer, Gene Ther. 14 (6) (2007) 465–475.
[33] W.T. Shi, F. Forsberg, P. Vaidyanathan, A. Tornes, J. Østensen, B.B. Goldberg, The influence of acoustic transmit parameters on the destruction of contrast microbubbles in vitro, Phys. Med. Biol. 51 (16) (2006) 4031–4045.
[34] S.H. Bloch, M. Wan, P.A. Dayton, K.W. Ferrara, Optical observation of lipid-and polymer-shelled ultrasound microbubble contrast agents, Appl. Phys. Lett. 84 (4) (2004) 631–633.
[35] P. Prentice, A. Cuschieri, K. Dholakia, M. Prausnitz, P. Campbell, Membrane disruption by optically controlled microbubble cavitation, Nat. Phys. 1 (2) (2005) 107.
[36] L.J. Jablonowski, N.T. Teraphongphom, M.A. Wheatley, Drug delivery from a multi-faceted ultrasound contrast agent: influence of shell composition, Molecular Pharm. 14 (10) (2017) 3448–3456.
[37] L.J. Jablonowski, D. Conover, N.T. Teraphongphom, M.A. Wheatley, Manipulating multifaceted microbubble shell composition to target both TRAIL-sensitive and resistant cells, J. Biomed. Mater. Res. Part A 106 (7) (2018) 1903–1915.
[38] J. Escoffre, J. Piron, A. Novell, A. Bouakaz, Doxorubicin delivery into tumor cells with ultrasound and microbubbles, Mole. Pharm. 8 (3) (2011) 799–806.
[39] R. Bekeredjian, H. Katus, H. Kuecherer, Therapeutic use of ultrasound targeted microbubble destruction: a review of non-cardiac applications, Ultraschall in der Medizin (Stuttgart, Germany: 1980) 27 (2006) 134.
[40] P.D. Bevan, R. Karshafian, E.G. Tickner, P.N. Burns, Quantitative measurement of ultrasound disruption of polymer-shelled microbubbles, Ultrasound Med. Biol. 33 (11) (2007) 1777–1786.
[41] L.J. Jablonowski, M.C. Cochran, J.R. Eisenbrey, N.T. Teraphongphom, M.A. Wheatley, Shell effects on acoustic performance of a drug-delivery system activated by ultrasound, J. Biomed. Mater. Res. Part A 105 (11) (2017) 3189–3196.
[42] L.J. Jablonowski, D. Alfego, J.I. Andorko, J.R. Eisenbrey, N. Teraphongphom, M.A. Wheatley, Balancing stealth and echogenic properties in an ultrasound contrast agent with drug delivery potential, Biomaterials 103 (2016) 197–206.
[43] R.W. Molinari, O.A. Khera, W.J. Molinari 3rd, Prophylactic intraoperative powdered vancomycin and postoperative deep spinal wound infection: 1,512 consecutive surgical cases over a 6-year period, Eur. Spine J. 21 (Suppl 4) (2012) S476–S482.
[44] C.L. Malone, B.R. Boles, K.J. Lauderdale, M. Thoendel, J.S. Kavanaugh, A.R. Horswill, Fluorescent reporters for staphylococcus aureus, J. Microbiol. Methods 77 (3) (2009) 251–260.
[45] C. Ketonis, S. Barr, I.M. Shapiro, J. Parvizi, C.S. Adams, N.J. Hickok, Antibacterial activity of bone allografts: comparison of a new vancomycin-tethered allograft with allograft loaded with adsorbed vancomycin, Bone 48 (3) (2011) 631–638.
[46] A.W. Bauer, W.M.M. Kirby, J.C. Sherris, M. Turck, Antibiotic Susceptibility Testing by a Standardized Single Disk Method, Am. J. Clin. Pathol. 45 (4_ts) (1966) 493–496.
[47] C. Basgul, T. Yu, D.W. MacDonald, R. Siskey, M. Marcolongo, S.M. Kurtz, Structure–property relationships for 3D-printed PEEK intervertebral lumbar cages produced using fused filament fabrication, J. Mater. Res. (2018) 1–12.
[48] B.M. Wu, S.W. Borland, R.A. Giordano, L.G. Cima, E.M. Sachs, M.J. Cima, Solid free-form fabrication of drug delivery devices, J. Controlled Release 40 (1) (1996) 77–87.
[49] N.S. Satarkar, J.Z. Hilt, Magnetic hydrogel nanocomposites for remote controlled pulsatile drug release, J. Control. Release 130 (3) (2008) 246–251.
[50] K. Sutani, I. Kaetsu, K. Uchida, Y. Matsubara, Stimulus responsive drug release from polymer gel: controlled release of ionic drug from polyampholyte gel, Radiation Phys. Chem. 64 (4) (2002) 331–336.
[51] M. Bikram, A.M. Gobin, R.E. Whitmire, J.L. West, Temperature-sensitive hydrogels with SiO2-Au nanoshells for controlled drug delivery, J. Control. Release 123 (3) (2007) 219–227.
[52] P. Costa, J.M.S. Lobo, Modeling and comparison of dissolution profiles, Eur. J. Pharm. Sci. 13 (2) (2001) 123–133.
[53] S. Dash, P.N. Murthy, L. Nath, P. Chowdhury, Kinetic modeling on drug release from controlled drug delivery systems, Acta Pol. Pharm. 67 (3) (2010) 217–223.
[54] A. Dokoumetzidis, P. Macheras, A century of dissolution research: from Noyes and Whitney to the biopharmaceutics classification system, Int. J. Pharm. 321 (1–2) (2006) 1–11.
[55] S. Friedman, N. Seaton, A corrected tortuosity factor for the network calculation of diffusion-coefficients, Chem. Eng. Sci. 50 (5) (1995) 897–900.
[56] A.A. Noyes, W.R. Whitney, The rate of solution of solid substances in their own solutions, J. Am. Chem. Soc. 19 (12) (1897) 930–934.
[57] L. Pismen, Diffusion in porous media of a random structure, Chem. Eng. Sci. 29 (5) (1974) 1227–1236.
[58] U. Schmidt, E.K. Schulte, Stains, Microscopic, Ullmann's Encyclopedia of Industrial Chemistry (2000).
[59] G. Baughman, S. Banerjee, T. Perenich, Dye Solubilities, in: A.T. Peters, H.S. Freeman (Eds.), Physico-chemical principles of color chemistry, Springer, Netherlands, 1996, pp. 145–195.
[60] K. Lewis, Multidrug tolerance of biofilms and persister cells, Curr. Topics Microbiol. Immunol. 322 (2008) 107–131.
[61] M.J. Rybak, C. Vidaillac, H.S. Sader, P.R. Rhomberg, H. Salimnia, L.E. Briski, A. Wanger, R.N. Jones, Evaluation of vancomycin susceptibility testing for methicillin-resistant Staphylococcus aureus: comparison of Etest and three automated testing methods, J. Clin. Microbiol. 51 (7) (2013) 2077–2081.
[62] V. Antoci Jr., C.S. Adams, N.J. Hickok, I.M. Shapiro, J. Parvizi, Antibiotics for local delivery systems cause skeletal cell toxicity in vitro, Clin. Orthop. Relat. Res. 462 (2007) 200–206.
[63] J. Siepmann, F. Siepmann, Mathematical modeling of drug delivery, Int. J. Pharm. 364 (2) (2008) 328–343.

Please cite this article as: L. J. Delaney, D. MacDonald, J. Leung et al., Ultrasound-triggered antibiotic release from PEEK clips to prevent spinal fusion infection: Initial evaluations, Acta Biomaterialia, https://doi.org/10.1016/j.actbio.2019.02.041

[64] Sigma-Aldrich, https://www.sigmaaldrich.com/content/dam/sigma-aldrich/docs/Sigma/Product_Information_Sheet/1/v1130pis.pdf accessed 11/29/2018 (2018).
[65] S. Prahl, Tabulated Molar Extinction Coefficient for Methylene Blue in Water, https://omlc.org/spectra/mb/mb-water.html accessed 11/29/2018 (2018).
[66] D.G. Leaist, The effects of aggregation, counterion binding, and added NaCl on diffusion of aqueous methylene blue, Can. J. Chem. 66 (9) (1988) 2452–2457.
[67] D. Sarkar, A. Bandyopadhyay, Adsorptive mass transport of dye on rice husk ash, J. Water Resour. Protection 2 (05) (2010) 424.
[68] V. Vadivelan, K.V. Kumar, Equilibrium, kinetics, mechanism, and process design for the sorption of methylene blue onto rice husk, J. Colloid Interface Sci. 286 (1) (2005) 90–100.
[69] H.-W. Fang, K.-Y. Li, T.-L. Su, T.C.-K. Yang, J.-S. Chang, P.-L. Lin, W.-C. Chang, Dip coating assisted polylactic acid deposition on steel surface: film thickness affected by drag force and gravity, Mater. Lett. 62 (21) (2008) 3739–3741.
[70] A. Vital, M. Vayer, T. Tillocher, R. Dussart, M. Boufnichel, C. Sinturel, Morphology control in thin films of PS:PLA homopolymer blends by dip-coating deposition, Appl. Surface Sci. 393 (2017) 127–133.
[71] S. Miyazaki, C. Yokouchi, M. Takada, External control of drug release: controlled release of insulin from a hydrophilic polymer implant by ultrasound irradiation in diabetic rats, J. Pharm. Pharmacol. 40 (10) (1988) 716–717.
[72] J. Kost, K. Leong, R. Langer, Ultrasound-enhanced polymer degradation and release of incorporated substances, Proc. Natl. Acad. Sci. USA 86 (20) (1989) 7663–7666.
[73] D. Levy, J. Kost, Y. Meshulam, R. Langer, Effect of ultrasound on transdermal drug delivery to rats and guinea pigs, J. Clin. Invest. 83 (6) (1989) 2074–2078.
[74] T.J. Evjen, E.A. Nilssen, S. Rognvaldsson, M. Brandl, S.L. Fossheim, Distearoylphosphatidylethanolamine-based liposomes for ultrasound-mediated drug delivery, Eur. J. Pharm. Biopharm. 75 (3) (2010) 327–333.
[75] V. Frenkel, Ultrasound mediated delivery of drugs and genes to solid tumors, Adv. Drug Deliv. Rev. 60 (10) (2008) 1193–1208.
[76] S. Hernot, A.L. Klibanov, Microbubbles in ultrasound-triggered drug and gene delivery, Adv. Drug Deliv. Rev. 60 (10) (2008) 1153–1166.
[77] S.L. Huang, Liposomes in ultrasonic drug and gene delivery, Adv. Drug Deliv. Rev. 60 (10) (2008) 1167–1176.
[78] N. Huebsch, C.J. Kearney, X. Zhao, J. Kim, C.A. Cezar, Z. Suo, D.J. Mooney, Ultrasound-triggered disruption and self-healing of reversibly cross-linked hydrogels for drug delivery and enhanced chemotherapy, Proc. Natl. Acad. Sci. USA 111 (27) (2014) 9762–9767.
[79] M.L. Fabiilli, C.G. Wilson, F. Padilla, F.M. Martin-Saavedra, J.B. Fowlkes, R.T. Franceschi, Acoustic droplet-hydrogel composites for spatial and temporal control of growth factor delivery and scaffold stiffness, Acta Biomaterialia 9 (7) (2013) 7399–7409.
[80] M. Schmitt, M.P. Walker, R.G. Richards, W.P. Bocchinfuso, T. Fukuda, D. Medina, F.S. Kittrell, K.S. Korach, R.P. DiAugustine, Expression of heregulin by mouse mammary tumor cells: role in activation of ErbB receptors, Mol. Carcinog. 45 (7) (2006) 490–505.

Please cite this article as: L. J. Delaney, D. MacDonald, J. Leung et al., Ultrasound-triggered antibiotic release from PEEK clips to prevent spinal fusion infection: Initial evaluations, Acta Biomaterialia, https://doi.org/10.1016/j.actbio.2019.02.041